Indo Proceedings of the XI DINAME, 28th February-4th March, 2005 - Ouro Preto - MG - Brazil
Edited by D.A. Rade and V. Steffen Jr.

PRESSURE FIELD INFLUENCE IN A HORIZONTAL ROTOR BEHAVIOR DUE TO THE ADDITION OF SEMI-CIRCULAR AXIAL GROOVES IN THE JOURNAL BEARING

Miguel Angelo de Carvalho Michalski
COPPE/UFRJ – LAVI – Sala I-130 – Centro de Tecnologia – Av. Jequitibá s/n – Cidade Universitária, Ilha do Fundão – Rio de Janeiro, RJ – CEP: 21945-970
michalski@ufrj.br

Moysés Zindeluk
COPPE/UFRJ – LAVI – Sala I-130 – Centro de Tecnologia – Av. Jequitibá s/n – Cidade Universitária, Ilha do Fundão – Rio de Janeiro, RJ – CEP: 21945-970
moyses@ufrj.br

Renato de Oliveira Rocha
Cepel – Centro de Pesquisa em Energia Elétrica – Av. Jequitibá s/n – Cidade Universitária, Ilha do Fundão – Rio de Janeiro, RJ – CEP: 21944-970
renato@cepel.br

Abstract. *The design of bearings and the characteristics of the lubricant are very important in the operation of a rotor machine. The geometry of a bearing can be very influential in the lubricant flow, and so in the final behavior of the machine. It happens because the pressure field created inside the bearing due to the rotor dynamics changes with the bearing geometry. Approaching that issue, in this paper an experimental study of the dynamic behavior of a horizontal rotor supported by journal bearings with semi-circular axial grooves is presented. A versatile workbench is used, making possible the analysis of a rotor model with different designs of bearings. Journal bearings are manufactured with a varied number of axial grooves. Different conditions can be simulated and using a numerical model the pressure field changes can be demonstrated, helping to understanding the phenomena.*

Keywords*: rotordynamics, journal bearings, axial grooves.*

1. Introduction

The combination of vibration and structural dynamics with hydrodynamic analysis brings up a great number of phenomena that deserve detailed investigation. In some cases, the models for numerical solutions are very well developed. In addition, a great number of experiments have been done and new experiments can suggest new ideas or simply confirm the theory.

The basic elements of a rotor are the shaft, the disks and the bearings and seals (Lalanne and Ferraris, 1998). Disks are generally modeled as rigid bodies and participate only in the kinetic energy of the system. The shaft can be represented by a beam and is characterized by strain and kinetic energies or, in simpler models, only the kinetic energy is taken into account when the shaft is considered as rigid as the disk. Seals and bearings add stiffness and viscous terms, assumed as known. Alternatively, they can also be modeled as external forces on the system.

Fluid film bearings can be usefully classified in terms of their rotor support mechanism, for the purpose of turbomachinery design analysis or monitoring and diagnosis or troubleshooting. (Vance, 1988). Fluid film bearings, one of the major types of bearings, can be sub-classified as hydrostatic or hydrodynamic bearings.

Both types need a fluid supply pressure, but in the second group, this pressure only needs to be high enough to maintain an ample supply of lubricant in the load-supporting clearance around the journal. The fluid support pressure is generated only by the motion of the journal and depends on the viscosity of the fluid. In cases of insufficient fluid supply, the rotor works under boundary, or starved (also known as pour) lubrication. This can happen in some small mechanisms or in some particular situations of industrial turbomachinery (Tanaka, 2000). The experimental model described in this paper uses journal bearings working under hydrodynamic lubrication. In this case, the lubricant supply is sufficient to prevent contact between the surfaces of the journal and the bearing.

The contracting oil film necessary to generate the pressure is obtained by a small lateral shift of the shaft or journal (Spots, 1984). In Fig. 1 an example of pressure field generation is given in a plain journal bearing. In this case, e represents the eccentricity between the center of the shaft and the bearing (in other words, the lateral shift of the shaft) and ω the velocity of the rotor.

The lubricant fluid is pulled by viscous shear into the high-pressure region produced by the eccentricity of the journal. The viscous shear is induced by the rotation of the journal (or bearing) that produces a relative velocity along

the film wall. In the high-pressure region, the fluid pressure rises, while in the low-pressure region, it decreases. The distribution of hydrodynamic pressure around the journal produces a force that reacts to the applied load.

Considering the design of the bearing, different models, from the simple plain bearing to sophisticated tilting pad journal bearings, can be found in the literature. Generally, the problem is to find the pressure field between the journal and the bearing and then the stiffness and damping coefficients. A derivation of a version of the Reynolds' equation is used to define the pressure field within a bearing as a function of its motion (Childs, 1993). In the next section, this equation will be introduced and discussed.

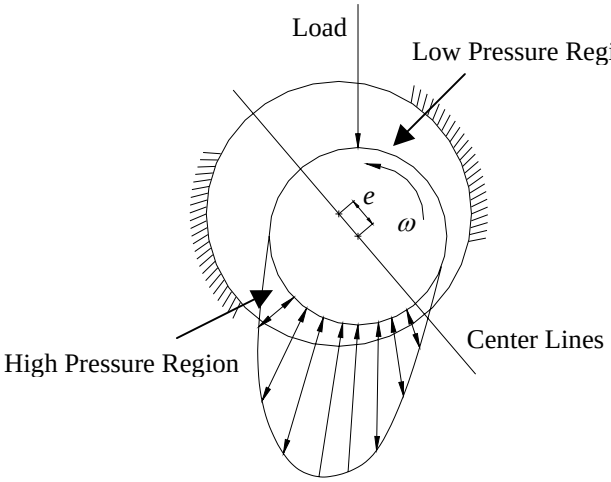

Figure 1. Pressure field generated in a plain journal bearing

2. The Pressure Field Mathematical Model

In order to build a mathematical model some simplifying standard assumptions are made with respect to the journal bearing, as a basis Reynolds' equation (Spots, 1984 and Kirk and Gunter, 1976).

(a) Newton's linear viscous model holds for the lubricant.
(b) The inertia effects of the lubricant can be neglected.
(c) Body forces can be neglected (the weight of the fluid in the film is small in comparison to the other acting forces).
(d) The lubricant is incompressible and the pressure across the film is constant.
(e) The density of the fluid is constant.
(f) Viscosity of the lubricant is constant throughout the film and is independent of changes in the temperature within the film.
(g) The film curvature with respect to the thickness can be neglected.

In Fig. 2 the geometry of a plain journal bearing is presented and it is possible to see the referential that follows the fluid and is present in Eq. (1). In addition, two new terms are given: R, the radius of the bearing and C_r, the radial clearance.

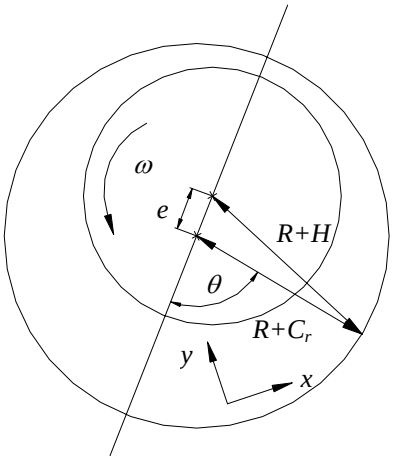

Figure 2. Plain journal bearing geometry

Considering also that H is the film thickness, P is the pressure field, r is the shaft radious and μ is the fluid viscosity, the Reynolds' equation is presented, in the form:

$$\frac{\partial}{\partial x}\left(H^3\frac{\partial P}{\partial x}\right)+\frac{\partial}{\partial y}\left(H^3\frac{\partial P}{\partial y}\right)=12\mu\left(\frac{\omega r}{2}\frac{\partial H}{\partial x}+\frac{\partial H}{\partial t}\right) \tag{1}$$

Circumferential coordinates are more suitable for the analysis of journal bearings. Reynolds' equation is represented in these new coordinates considering that the circumferential variable x is replaced by $R\theta$. The angle θ is illustrated in Fig. 2 and it is a counterclockwise rotation originated at the line of centers.

$$\frac{1}{R^2}\frac{\partial}{\partial\theta}\left(H^3\frac{\partial P}{\partial\theta}\right)+\frac{\partial}{\partial y}\left(H^3\frac{\partial P}{\partial y}\right)=12\mu\left(\frac{1}{R}\frac{\omega r}{2}\frac{\partial H}{\partial\theta}+\frac{\partial H}{\partial t}\right) \tag{2}$$

To obtain useful solutions, two successful alternative approaches have been employed: Reynolds' equation simplification for especial cases of practical interest, resulting in a functional solution or the reformulation of the equation into finite-difference or finite-element form, resulting in a numerical solution. (Vance, 1988).

In addition, two special limiting cases are used: the Ocvirk Bearing Solution, for short bearings and the Sommerfeld Bearing Solution, for long bearings. Considering that L is the bearing length and D its diameter, when $L/D < ½$ the bearing is considered short and when $L/D > 1$, the bearing is considered long.

In this paper, the first case was used. The Ocvirk model gives a reasonably good definition of bearing-reaction direction but predicts an erroneously large magnitude. The error in the magnitude increases sharply for high eccentricity ratios (Childs, Moes and van Leeuwen, 1997). In this case, the Reynolds' equation is simplified, represented by the Eq. (3) below. A direct integration in y can render the equations' solution (Meggiolaro, 1996).

$$\frac{\partial}{\partial y}\left(H^3\frac{\partial P}{\partial y}\right)=12\mu\left(\frac{1}{R}\frac{\omega r}{2}\frac{\partial H}{\partial\theta}+\frac{\partial H}{\partial t}\right) \tag{3}$$

At this point, for each design of bearing, the equation has a different solution. To obtain the pressure field it is necessary to know the film thickness as function of y and θ. Once the orbit inside the bearing is known, as well as the bearing geometry, the thickness will be simply the difference between the geometry and the orbit. To set an example of the theory, a general orbit is considered, as presented in Fig. 3, with two different journal bearings. In this case, a simple equation can describe the orbit and the bearing geometry.

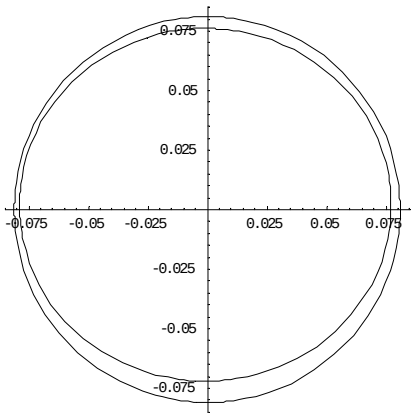

1. Plain Journal Bearing

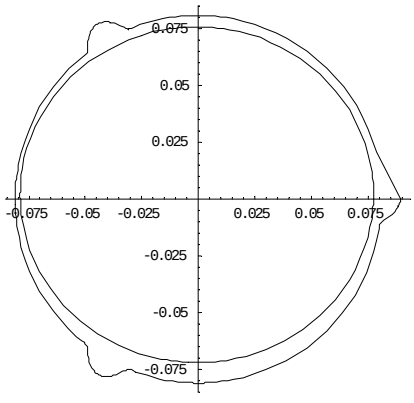

2. Journal Bearing with 3 Grooves

Figure 3. Examples of orbits in different Journal Bearings.

The pressure field calculated in the center of the journal bearing as a function of θ, for both examples, is presented in Fig. 4. Here, the Sommerfeld's Boundary Conditions for a circular bearing were considered (Meggiolaro, 1996), only as an example.

In the second case shown, with the grooves added to the journal bearing, peaks of pressure appear related to the positions of the semi-circular axial grooves. The magnitude of these peaks is higher than the rest of the integrated pressure field, generating higher forces very concentrated in specific positions. On the other hand, the amplitude fall of the pressure in these grooves is as huge as its rise.

The presence of negative pressures does not have a physical equivalence. Actually, the cavitation effects vaporize the oil film, not allowing the presence of vacuum or negative pressures. Therefore, the Gümbel or Reynolds Boundary

Conditions could be more appropriate. In Fig. 5 are shown the same pressure fields from Fig. 4 but with the Gümbel Conditions.

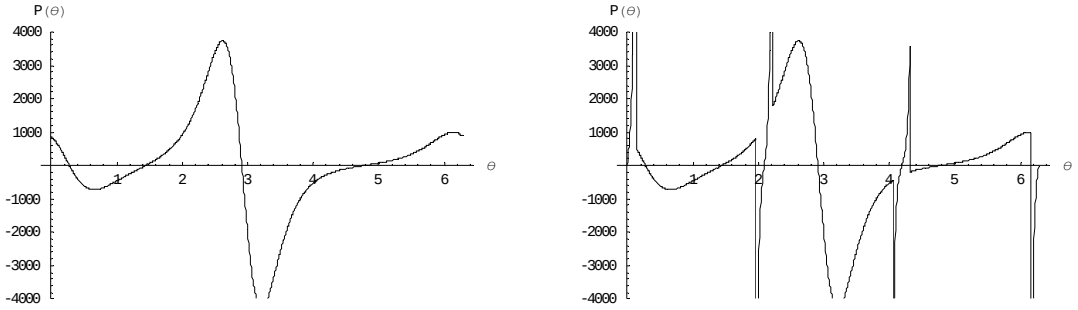

1. Plain Journal Bearing 2. Journal Bearing with 3 Grooves

Figure 4. Pressure Fields considering the Sommerfeld's Boundary Conditions.

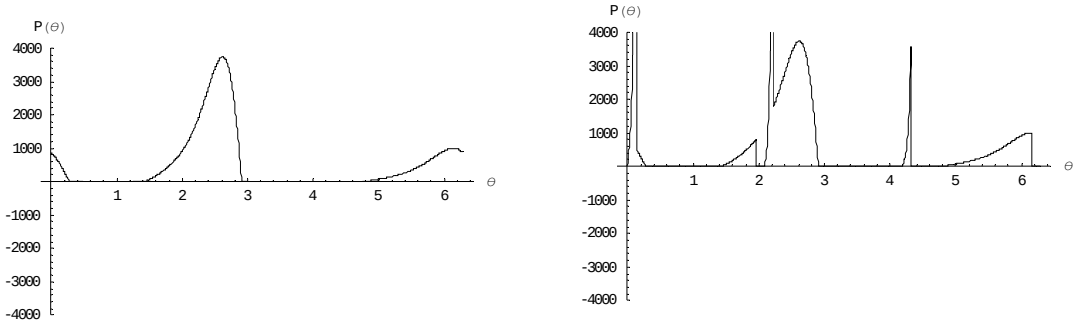

1. Plain Journal Bearing 2. Journal Bearing with 3 Grooves

Figure 5. Pressure Fields considering the Gümbel's Boundary Conditions.

3. The Experimental System

The experiment has been based on a rotor (Fig. 6) composed by a shaft, two disks and two journal bearings. The shaft has a total length of 540 mm and it is made of solid steel SAE 1045; the center part has a length of 400 mm and diameter of 12 mm; the extremities are symmetric: the length is 70 mm and the diameter is 8 mm for both. The disks, in the same material, are fixed on the shaft with a distance of 200 mm and 375 mm respectively from the left end of the shaft; their diameter is 115 mm and the thickness is 15 mm; they also have 36 holes in order to balance (or unbalance).

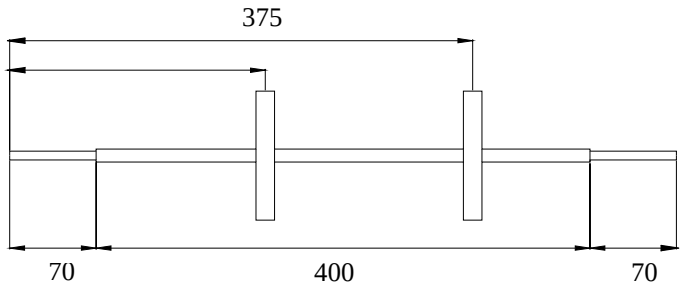

Figure 6. Rotor Simplified Scheme

The bearings stand about 55 mm from each end of the axis. They were manufactured in bronze with an inside diameter near 8.1 mm and 8.0 mm length. They are placed in supports and two lids are used to lock each bearing inside the support.

Oil is supplied from the top of each support and extracted from both lids, through flexible pipes with a diameter of ¼ inch.

The supports are attached to a cast iron base that assures the alignment between the bearings. The cast iron base is considered an inertial reference to the rotor, as its vibration amplitude is much smaller than the amplitude of the rotor. The block weighs is about 170 kgf and the rotor about 2,8 kgf.

The system is driven by an electric motor with variable speed. Inductive analog sensors (Balluff BAW 018-PF-1-K) connected to an oscilloscope HP 54603B measure the orbits at the disks. Two sensors are perpendicularly positioned to the disk, in the radial direction, with 90º between them. A third sensor can be used to acquire the displacement in the axial direction (Abrantes and Michalski, 2002). The sensors were calibrated in order to work in their linear range. An aluminum disk with a single hole positioned in the electric motor shaft trigger the signals. By this way all the signals are acquired considering the same start position.

In Fig. 7, two bearings are presented. The first one, a plain journal bearing out of the support and the second one, a journal bearing with three axial-grooves positioned in the support.

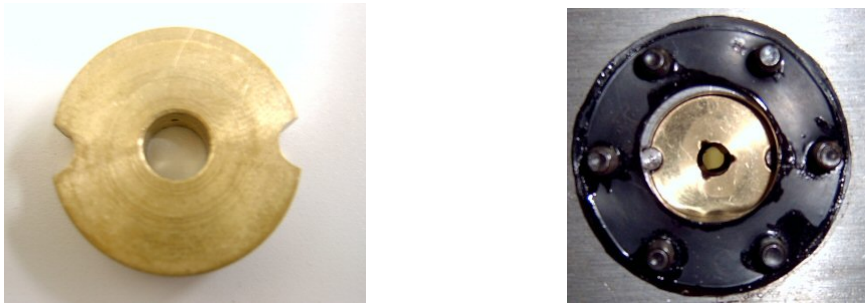

Figure 7. Bearings

A general view of the rotor is presented in Fig. 8, with a detail of the workbench with the sensors and disks in evidence.

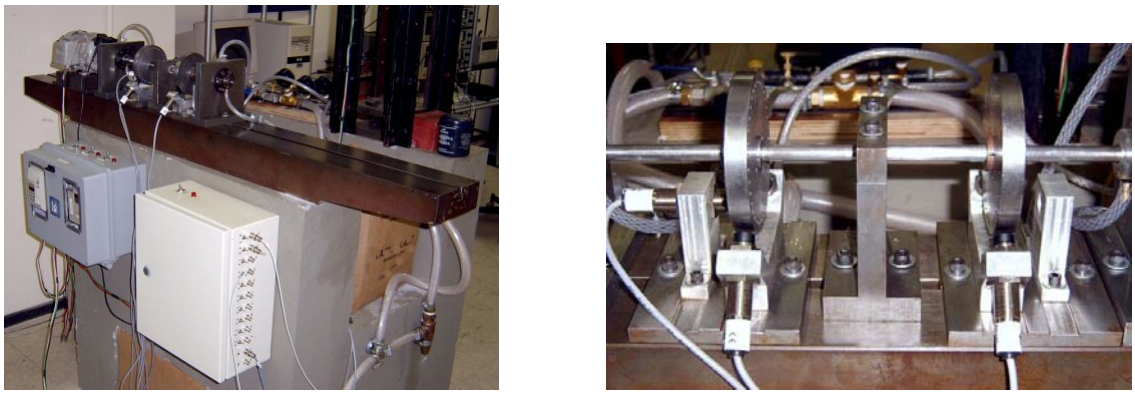

Figure 8. Rotor general view and detail

4. The Experimental Results and Analysis

Data acquisition was performed at three different speeds for each journal bearing. The values correspond to the orbits of the two disks mounted in the rotor.

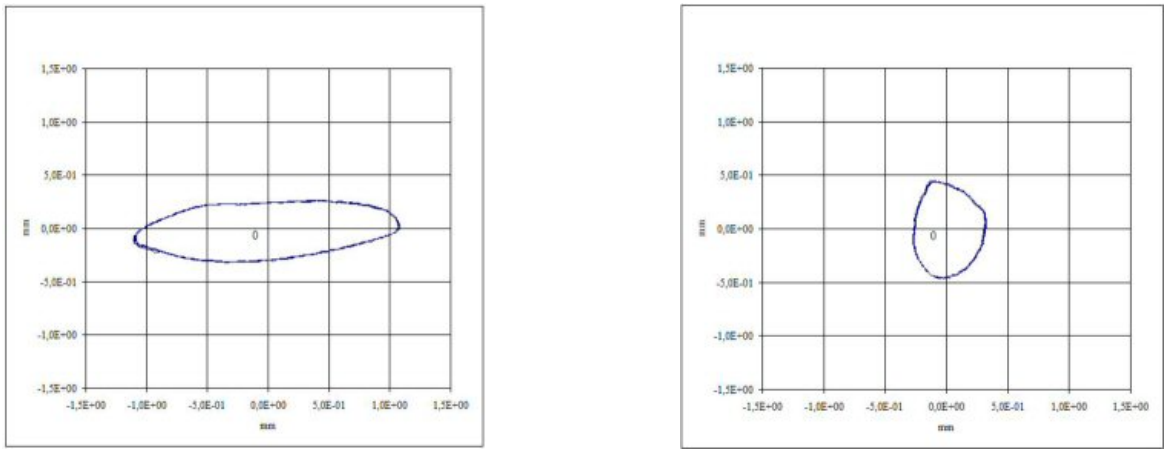

40,75 Hz

43,5 Hz

Figure 9. Orbits near the first critical speed

The first critical speed of the rotor was experimentally obtained and is about 40 to 44 Hz for both configurations. This can be shown with the two orbits presented in Fig. 9, taken from the rotor configuration with the three axial grooved journal bearing. The first one was taken from the first disk in a rotational speed of 40,75 Hz. And the second one was taken from the same disk but with a rotational speed of 43,5 Hz. In both pictures, the displacements (horizontal and vertical) are in millimeters.

It is possible to see the phase between the major axes from each ellipse (90º degrees), demonstrating the critical speed crossing (Lalanne, 1998).

The three basic speeds were 1,1 Hz, 30 Hz and 60 Hz. With the first one, it is possible to measure the rotor run-out. The second one corresponds to a speed under the first critical and the third one corresponds to a speed above the critical. A table with signals taken from the first disk is given in Fig. 10

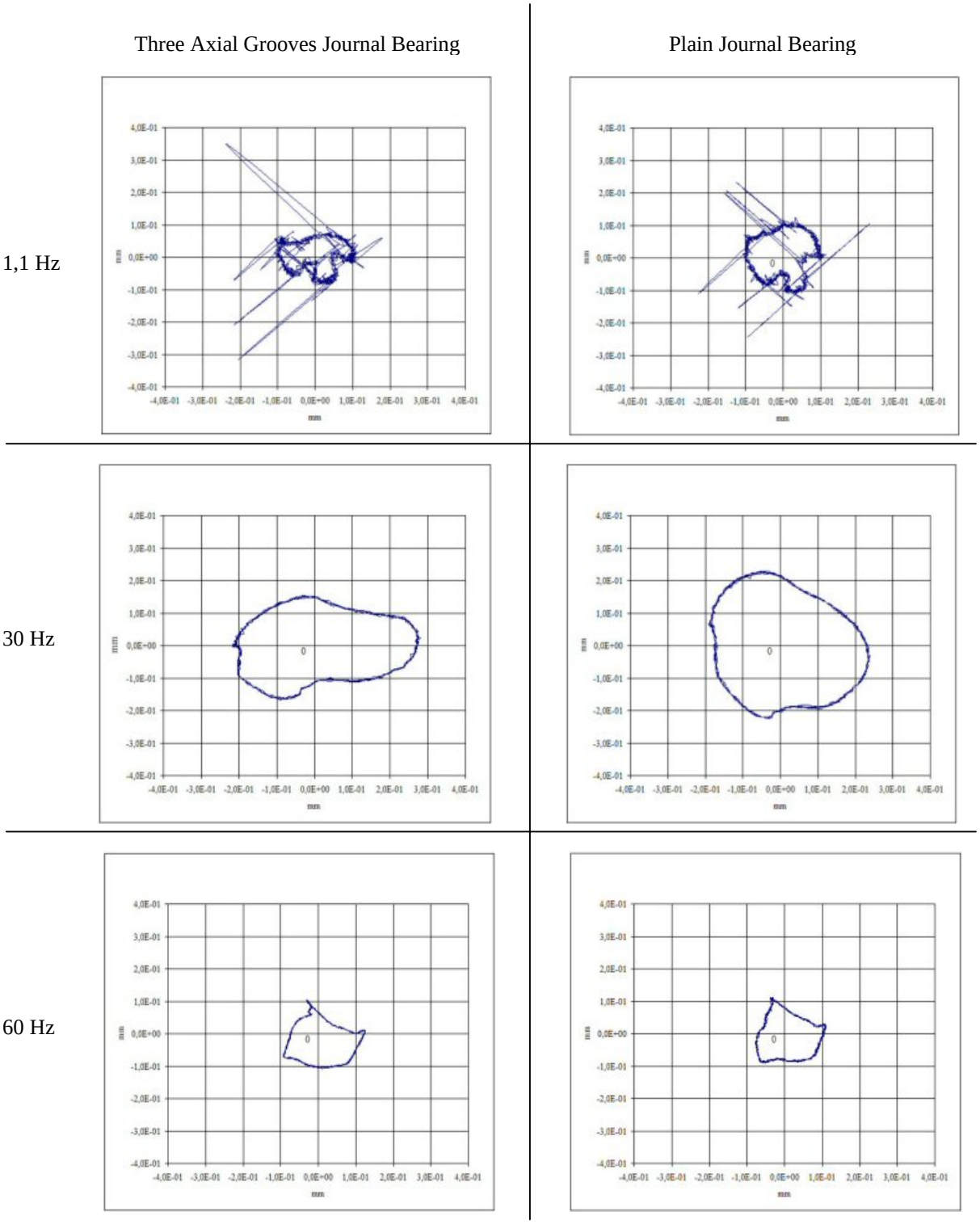

Figure 10. First Disk Orbits

In the first line of the presented table, it is possible to see, a great number of undesirable peaks. They are generated by a high frequency noise from the motor speed control. A low pass filter could be used but to prevent signal deformations this idea was not applied. This noise is not present in the 30 Hz and 60 Hz orbits because an average value was used to trace the orbit.

The signals in the frequency domain were also observed and, for all the situations described, an outstanding peak corresponding to the rotational frequency and some harmonics characterizes the graphic. An example is the FFT from the sensor number one, placed in the first disk, with a rotational speed of 30 Hz, in Fig. 11.

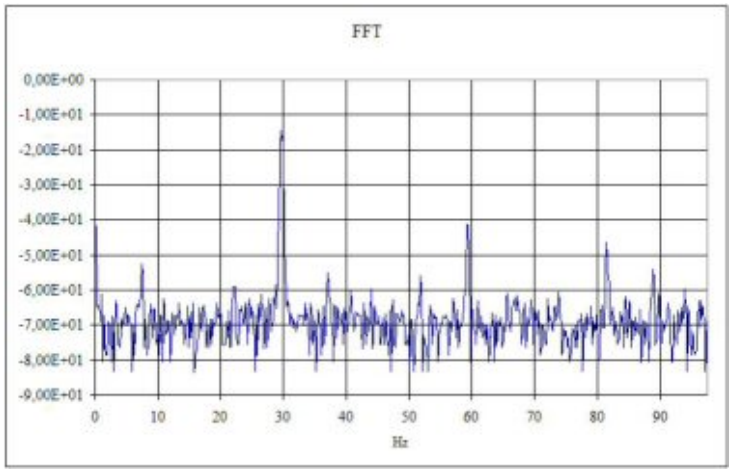

Figure 11. Example of Signal FFT

Observing the graphics of Fig. 10, the most important difference noticed is that with the grooved journal bearing the displacement in the vertical direction is smaller than the same displacement when the plain bearing is used.

Another situation was induced: The behavior of the rotor near a speed twice the value of the first critical. In this case, the rotor was driven up to 100 Hz. With the plain journal bearing nothing special was observed. However, with the three axial grooves journal bearing instability was observed. As a matter of fact, the center of the orbit around 87 Hz was not stable, apparently moving between two defined positions. In Fig. 12 the orbit in this speed is shown.

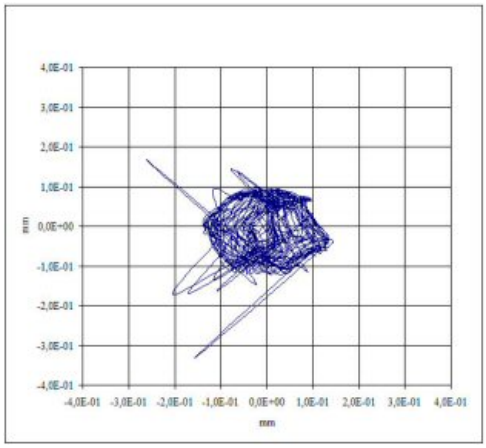

Figure 12. Unstable Orbit

In this case, an average value was not used in order to preserve the instability. So, the noise is visible but does not interfere in the phenomenon. In Fig. 13 the FFT signal acquired with sensor number one is shown.

It is possible to see in the frequency domain that near the first critical speed there are two great peaks. This shows a self-excited vibration of the system with a frequency near the first rotor critical speed, when no external forces are present but an internal feedback mechanism transferring the rotational energy into vibrations, similar to the oil whirl and oil whip phenomena (Muszynska, 1985).

The rotational energy refers to the oil film, whose rotational average speed is near half of the shaft rotational speed (Meggiolaro, 1996). Therefore, when the rotor works with a frequency twice the first critical frequency the oil film speed is almost at the first critical value.

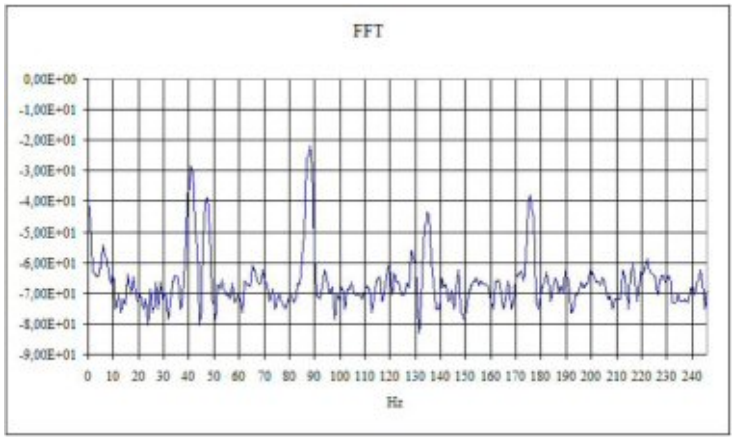

Figure 13. FFT at 87 Hz with three grooved journal bearing

Considering that the oil supply did not change from one bearing to the other, its pressure and flow are the same, the test speeds and conditions were the same, the presented differences in the rotor assemblies show that, first, the rotor was more susceptible to its own weight down force with the grooved journal bearings, and, second, it was also more susceptible to instability problems in speeds near twice the first critical.

Apparently, the grooves presence gave the rotor light radial load characteristics. However, in horizontal rotors, generally the radial load (weight) is enough to keep the oil film stable (Muszynska, 1985).

5. Conclusions

This paper presents some pressure field influence in a horizontal rotor behavior. Two journal-bearing models were used in order to compare the results between them, working with the rotor at several speeds (1,1 Hz, 30 Hz, near 43 Hz, 60 Hz and up to 100 Hz). The first model was a simple plain bearing and the second one a three semi-circular axial grooved journal bearing

A mathematical model was also used to show the theoretical difference between the pressure fields inside the bearings but it was not possible to show the real field in the experimental cases. However, the differences between the models were experimentally noticeable.

When the rotor worked in lower speeds, the radial load pushed the rotor down and near 87 Hz (the first critical was experimentally observed near 43 Hz) the rotor presented an unstable behavior when the grooved journal bearings were used. As a matter of fact, the orbit in this case oscillated between two different center points. When the plain bearing was used, the orbits were always very well defined, as expected for a horizontal rotor.

The cause of the instability problem noticed is apparently the same as the one in oil whirl and oil whip, as occurs in rotors with low radial load or, in other words, low eccentricity. The continuity of this work can bring new evidences of this unstable behavior and help with a mathematical model to simulate some instability problems or the rotor working with different types of journal bearings.

6. Acknowledgements

The authors would like to thank Ranny Nascimento, Anderson Pereira and Fábio Frade. Their help was essential to this work. We hope to always count on them and return the favor someday.

7. References

Abrantes M. V. G. D. and Michalski, M. A. C., 2002, “Projeto e Construção de uma Bancada Experimental para Estudos em Dinâmica de Rotores Horizontais”, Graduation Final Project, EE – UFRJ, Rio de Janeiro, RJ, Brasil.

Childs, D., 1993, “Turbomachinery Rotordynamics – Phenomena, Modeling, and Analysis”, John Wiley and Sons.

Childs, D., Moes, H. and van Leeuwen, H., 1977, “Journal Bearing Impedance Descriptions for Rotordynamics Applications”, Transactions of ASME, Journal of Lubricant Technology, April 1977.

Kirk, R. G. and Gunter, E. J., 1976, “Short Bearing Analysis Applied to Rotor Dynamics – Part I: Theory”, Transactions of ASME, Journal of Lubricant Technology, January 1976.

Kirk, R. G. and Gunter, E. J., 1976, “Short Bearing Analysis Applied to Rotor Dynamics – Part II: Results of Journal Bearing Response”, Transactions of ASME, Journal of Lubricant Technology, April 1976.

Lalanne, M. and Ferraris, G., 1998, “Rotordynamics Prediction in Engineering”, Second Edition, John Wiley and Sons.

Meggiolaro, M. A., 1996, “Modelagem de Mancais Hidrodinâmicos na Simulação de Sistemas Rotativos”, M.Sc. Thesis, Mechanical Engineering Department, PUC-Rio.

Muszynska, A., 1986, “Whirl and Whip – Rotor/ Bearing Stability Problems, Journal of Sound and Vibration, Vol. 110, No. 3, pp. 443 – 462.
Spots, M. F., 1984, “Design of Machine Elements”, Fourth Edition, Pretice-Hall.
Tanaka, M., 2000, “Journal Bearing Performance Under Starved Lubrication”, Tribology International, Vol.33, pp. 259-264.
Vance, J. M., 1988, “Rotordynamics of Turbomachinery”, John Wiley and Sons.

8. Responsibility notice

The authors are the only responsible for the printed material included in this paper.